Using X-ray diffraction for studying the effect of modulation and machining parameters on deformation level in brass particulate produced by modulation assisted machining

Ravinder Singh Joshi[a1] [c1], Harpreet Singh[a1]

[a1] School of Mechanical, Materials and Energy Engineering, Indian Institute of Technology Ropar, Rupnagar, Punjab, India

In present investigation, effect of modulation and machining parameters on deformation level of the chips produced during modulation assisted machining (MAM) has been studied. It is shown that disruption in tool-chip contact during modulation assisted machining helps in the formation of discrete chips. Size and shape of the particles produced in MAM can be controlled by varying modulation and machining conditions. Particulates of different shapes and sizes ranging from 100 μm to 5 mm with an aspect ratio of ~10 were produced using MAM. The morphology of the particulates produced was characterized by scanning electron microscope (SEM). Deformation in chip particulates was investigated using X-Ray diffraction. The crystallite size and internal strain in particulates were evaluated using Scherrer and Williamson-Hall methods respectively. The crystallite size of the particulates was found to decrease with decrease in their size, whereas internal strain in particulates was observed to increase with decrease in their size. Furthermore, the length of particulates was observed to decrease with an increase in the ratio of frequency of modulation (f_m) to frequency of workpiece rotation (f_w). However, the corresponding change in microstrain and crystallite size was insignificant with change in this ratio.

Key words: Modulation assisted machining; Particulate production; X-Ray diffraction; Crystallite size; Microstrain.

[c1] a) Corresponding author email**:** ravindersj@iitrpr.ac.in

https://doi.org/10.1017/S088571561300095X Published online by Cambridge University Press

I. INTRODUCTION

Metal powders are generally produced by several routes, such as physical, mechanical and chemical. Typically shape, size and internal structure of the particles produced are process dependent (Lenel, 1980). There is a very little control on particle size distribution and internal structure within a process. In modulation assisted machining (MAM), modulations are superimposed on the cutting tool to move it relative to the material being machined and cause periodic separation between cutting tool and workpiece. In this way, each separation between the cutting tool and the workpiece produces a chip. The shape and size of the chips (particulates) depend firstly, on the length of time the cutting tool is in contact with the workpiece during each modulation cycle. Secondly, the area of contact between the tool and workpiece also influences these physical characteristics of the chips. Length of time and area of contact can further be controlled by different modulation and machining conditions. MAM can be scaled down to produce powder-like particles (Mann et al., 2007). By varying the machining and modulation parameters during MAM, the shape and size of the particles can be controlled. Furthermore, internal structure of the particles depends on the level of deformation in the particles. This level of deformation in particles can further be controlled by changing the rake angle, modulation and machining conditions. The main advantage of MAM as compared to its counterparts is the production of particles with narrow size distribution, as well as, control on their microstructure. Moreover, application of oscillations by piezoelectric actuators in machining reduces the cutting forces and burr formation, which further reduces energy consumption. These features make modulation assisted machining an energy efficient process, which is a step towards sustainability (Joshi and Singh, 2011).

II. EXPERIMENTAL METHOD

A schematic of MAM system used for the particulate production in the present investigation is shown in Fig. 1. A three axis computer numeric control (CNC) machine was used as a machining platform for this study. TriboMAM (A patented tool holder of M4Sciences) (Mann et al., 2009) was used for superimposing vibration to the tool motion, which was retrofitted on the CNC machine. Piezoelectric actuator used in the TriboMAM is able to impose a modulation of amplitude and modulation frequency upto 0.2 mm and 1000 Hz respectively. A brass tube of diameter 25.4 mm and wall thickness 1.2 mm was used as a workpiece material. A single point cutting tool (HSS) was used for the machining experiments. The experimental conditions for the

https://doi.org/10.1017/S088571561300095X Published online by Cambridge University Press

study included a frequency range of 10 - 20 Hz for workpiece rotation (f_w), a feed (h_0) of 0.0182 mm/rev with varying depth of cut values as 700, 500, 300 and 150 µm. The chips developed at different conditions were collected on a paper sheet and examined under tool maker's microscope (Radical) and scanning electron microscope (JEOL6610LV) to study their morphology. The size of the chip refers to its longitudinal dimension (length) in the present study. Deformation level in the produced particulates was evaluated by X-ray diffraction (XRD) approach. XRD measurements were performed using a Panalytical X-Pert Pro diffractometer (θ - 2θ) equipped with Cu-Kα radiation (λ = 1.5418 Å). Several frequency ratios (f_m/f_w) were imposed to verify the discrete chip model (Mann et al., 2007) with contact disruption and deformation strain in the chip particulates. f_m refers to the frequency of modulation in this study.

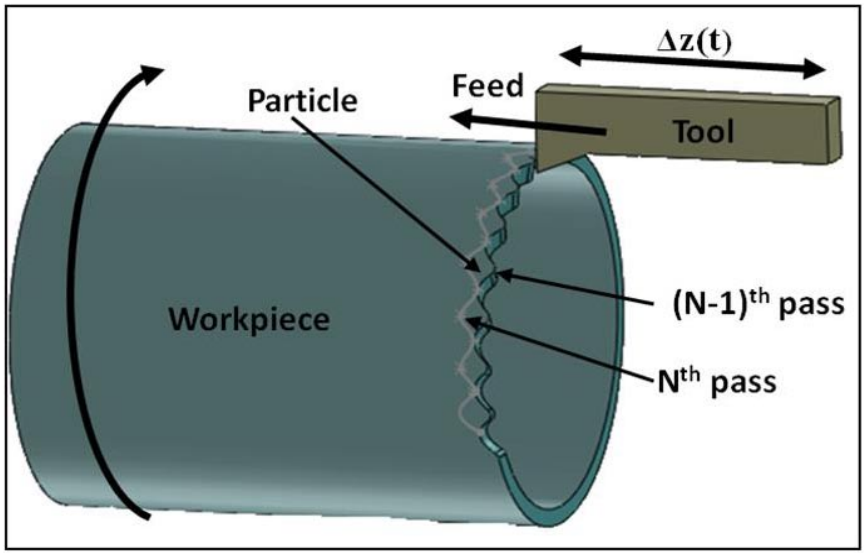


Figure 1: Schematic of MAM system used for particulate production

It is well known that in X-ray diffractogram broadening of the line is influenced by the internal strains and crystallite size. In order to obtain internal strain, Williamson-Hall method was used (Williamson and Hall, 1953), whereas Scherrer method was used to calculate crystallite size. In the Williamson-Hall method, the analysis includes the following two steps:

First step: The integral breadth of the peak was considered as width (β_{exp}). Integral breadth is the ratio of the area under the peak to the height of the peak. For finding out the instrumental broadening (β_{inst}), polycrystalline silicon standard was used (Biju et al., 2008). Then peak breadths (B) due to sample (size + strain) were calculated according to Gaussian profile:

https://doi.org/10.1017/S088571561300095X Published online by Cambridge University Press

$$B^2 = \beta_{exp}^2 - \beta_{inst}^2 \quad (1)$$

Second step: The internal strain was obtained using Williamson-Hall equation (2). Internal strain was the slope of a line fitted between points of plot between $B\cos\theta$ and $\sin\theta$

$$B\cos\theta = (k\lambda/D) + 2\varepsilon \sin\theta \quad (2)$$

Where D is the coherent scattering length (crystalline size); K is a constant whose value is approximately 0.9; B the integral width of the sample (in rad) calculated in the first step and ε is the inhomogeneous internal strain (in %).

Scherrer formula (3) was used to calculate the crystallite size

$$D = k\lambda / B\cos\theta \quad (3)$$

In this case, the peak width (in rad) was determined as the full width at half-maximum (FWHM) by a Gaussian fitting.

When a material is deformed the Bragg reflections detected with XRD can be affected in two ways. First the peaks will shift in the presence of mean strains. Second, the breadth and shape of the peaks can change for two reasons: (i) the size of diffracting elements (e.g. the grain size) changes; and (ii) changes in inhomogeneous strain (micro-strain). Possible sources of inhomogeneous strain include lattice dislocations, grain boundary defects and intracrystalline gradient such as high-dislocation-density walls surrounding low-dislocation-density cell interiors (Ungar et al., 2001). The four most intensive reflection peaks of the samples were used in the line broadening analysis. Then the internal strain was estimated from the Williamson-Hall method. The crystallite size was determined by Scherrer formula. To calculate the crystallite size the peak width was considered as the full width at half-maximum (FWHM).

III. RESULTS AND DISCUSSION

A. Deformation level in different sized chip particulates and bulk of brass

Particulates of several shapes and size range (100 µm - 5 mm) with an aspect ratio of ~10 were produced using MAM. For the deformation analysis, the particulates of size 1200, 700, 400 and 100 µm were used. The modulation and machining conditions used for the production of the above said particulates are tabulated in Table I. Figure 2 shows the XRD profiles of different particle-sized powders of brass and bulk brass. It is clear from the figure that the peak shape is

https://doi.org/10.1017/S088571561300095X Published online by Cambridge University Press

symmetric on the onset of powder production (Bulk brass). Furthermore, the particle size decreases, the breadth and asymmetry are found to increase. This may be attributed to the fact that the large grain may deform plastically, whereas the smaller grains remain primarily elastic leading to inhomogeneous deformation in the particulates (Lonardelli et al., 2009). The crystallite size of powder is found to decrease with the decrease in powder size. This may be explained on the basis of a decrease in the coherent scattering volumes due to increase in dislocation density, stacking faults, twins and related defects during deformation (Lonardelli et al., 2009). It has also been observed that as the particle size decreases, there is an increase in the microstrain. This shows that the deformation in the particle of 100 μm size is large in comparison with that in the particle of 1200 μm size. Inhomogeneous strain in the particles may primarily due to increase in dislocation density. Therefore, the properties of particulates produced are expected to be better than bulk.

Table I: Machining and modulation conditions for machining brass to different sized chip particles

Particle Size (μm)	1200	700	400	100
Workpiece Diameter (mm)	25	25	25	6
Speed (f_w) (rpm)	600	300	180	180
Feed (h_0)(mm/rev)	0.018	0.018	0.018	0.018
Depth of Cut (μm)	500	300	200	50
Vibration Amplitude (A) (mm)	0.015	0.015	0.020	0.020
Vibration Frequency (f_m) (Hz)	275	852.5	836	836

https://doi.org/10.1017/S088571561300095X Published online by Cambridge University Press

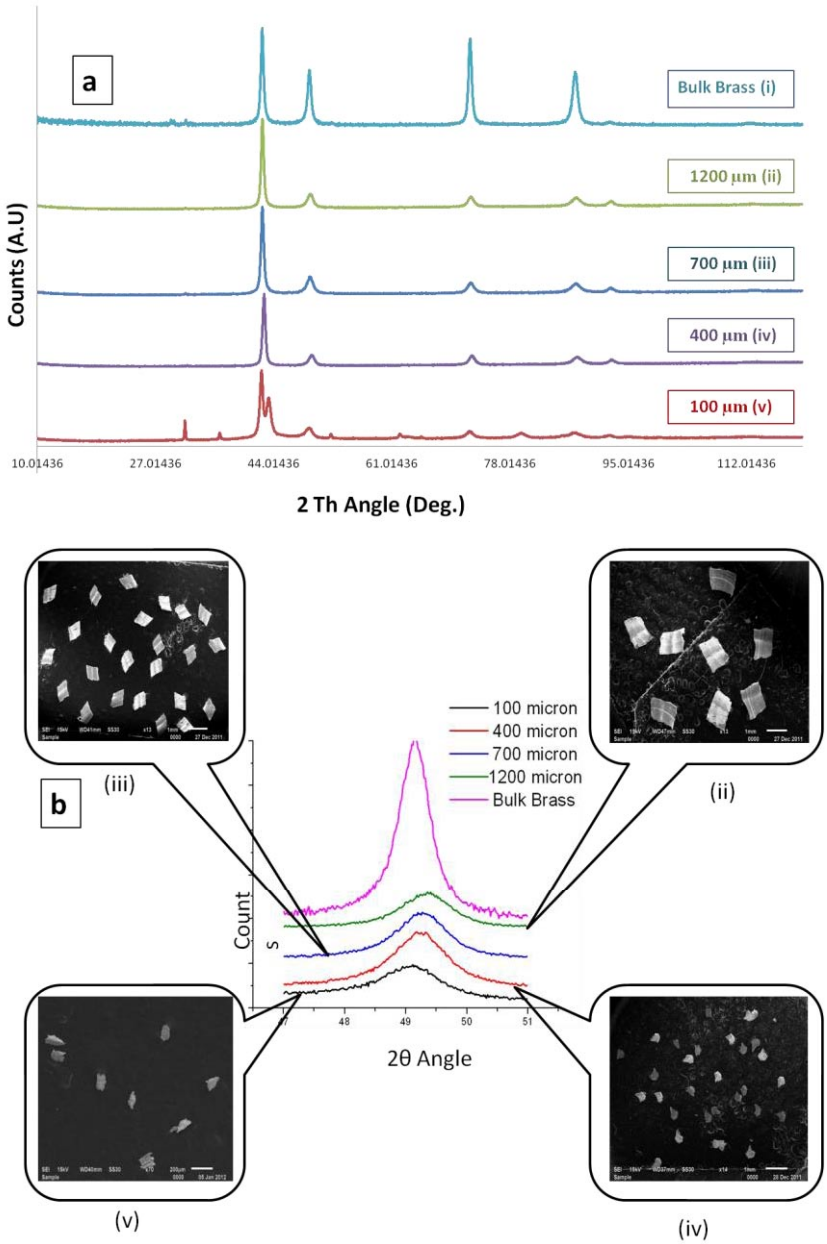


Figure 2: XRD profiles of brass subjected to modulation-assited machining (MAM) under several modulation and machining conditions: (a) Full XRD profiles (b) Details of peak shift at 49.093^{o} and particulates' morphology. (i) Bulk brass (ii)-(v) Chips having average size 1200, 700, 400 and 100 µm respectively

Fig. 3b shows the evolution of crystallite size with particulates size obtained by Scherrer methods. It is evident that with decrease in chip particulate size, the crystallite size also decreases, while the internal strain increases (Fig. 3a). In the case of 100 µm-sized powders, the internal strain is increased from 0.007 to 0.06 approx. However, crystallite size of the powder is decreased from 24 to 8 nm. This change in crystallite size and microstrain may be attributed to the severe plastic deformation (SPD) taking place during MAM. This SPD increases the defects

https://doi.org/10.1017/S088571561300095X Published online by Cambridge University Press

in chip particulates, thereby changing the microstrain and the crystallite size of the particulates. Similar behaviour has been reported during ball milling by several groups (Sánchez et al., 2007; Pourghahramani et al., 2008; Lemine 2009). They also observed a clear reduction in crystallite size with decrease in particle size for a longer milling time.

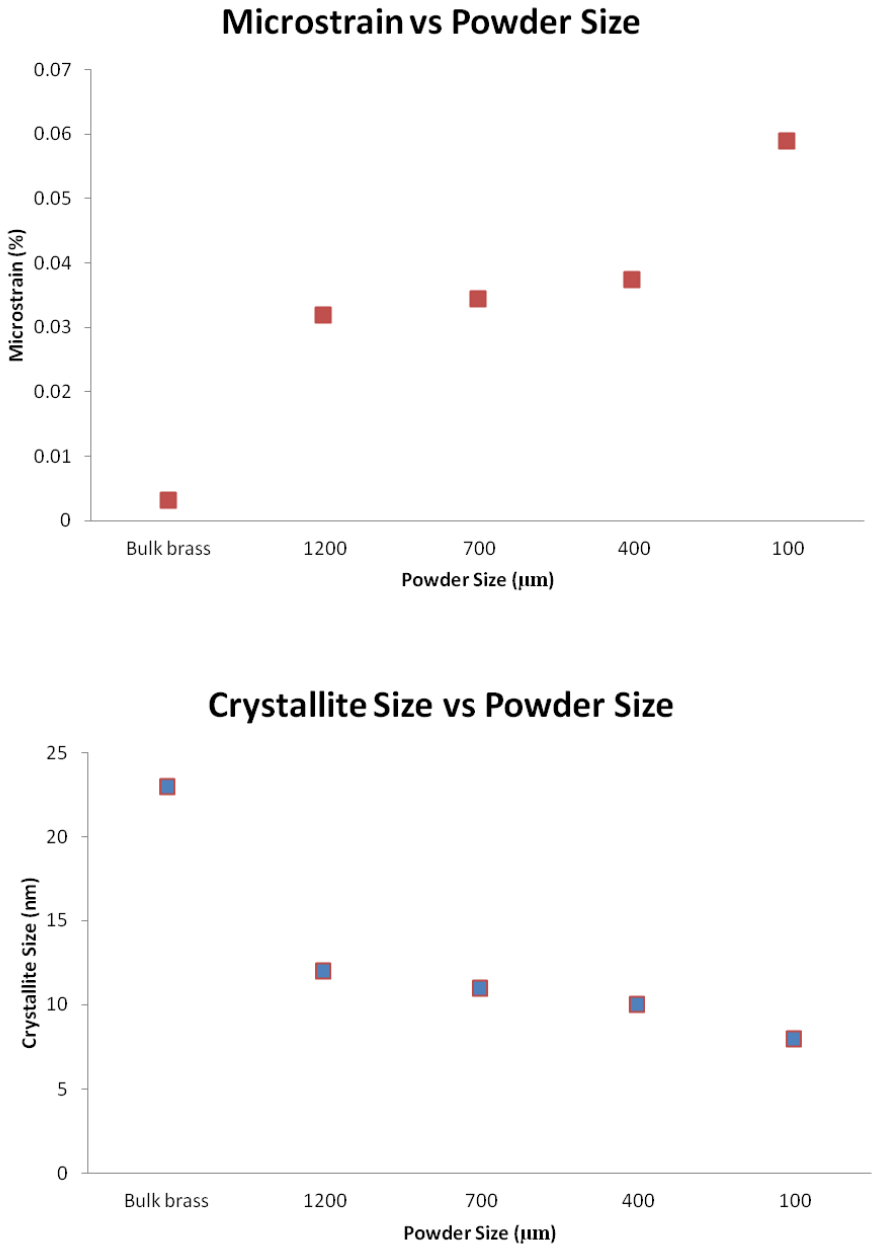


Figure 3: Plots showing effect of chip particulates size on (a) Microstrain, (b) Crystallite size

https://doi.org/10.1017/S088571561300095X Published online by Cambridge University Press

B. Effect of f_m/f_w on chip morphology and level of deformation in chip particulates

For this analysis, the frequency of workpiece rotation (f_w) and other machining parameters were kept constant. The frequency of modulation (f_m) was changed to achieve different values of f_m/f_w ratio. The particulates produced at different f_m/f_w ratios are shown in Fig. 4. It is seen that as f_m/f_w is increased, the chip lengths become increasingly smaller, consistent with discrete chip segments being formed more frequently at the rate of f_m/f_w per revolution.

Also, when f_m/f_w was set equal to integer values, continuous chips of constant thickness were produced as shown in the bottom row of Fig. 4. These observations are again consistent with predictions of the chip formation model for turning proposed by Mann et al. (2007).

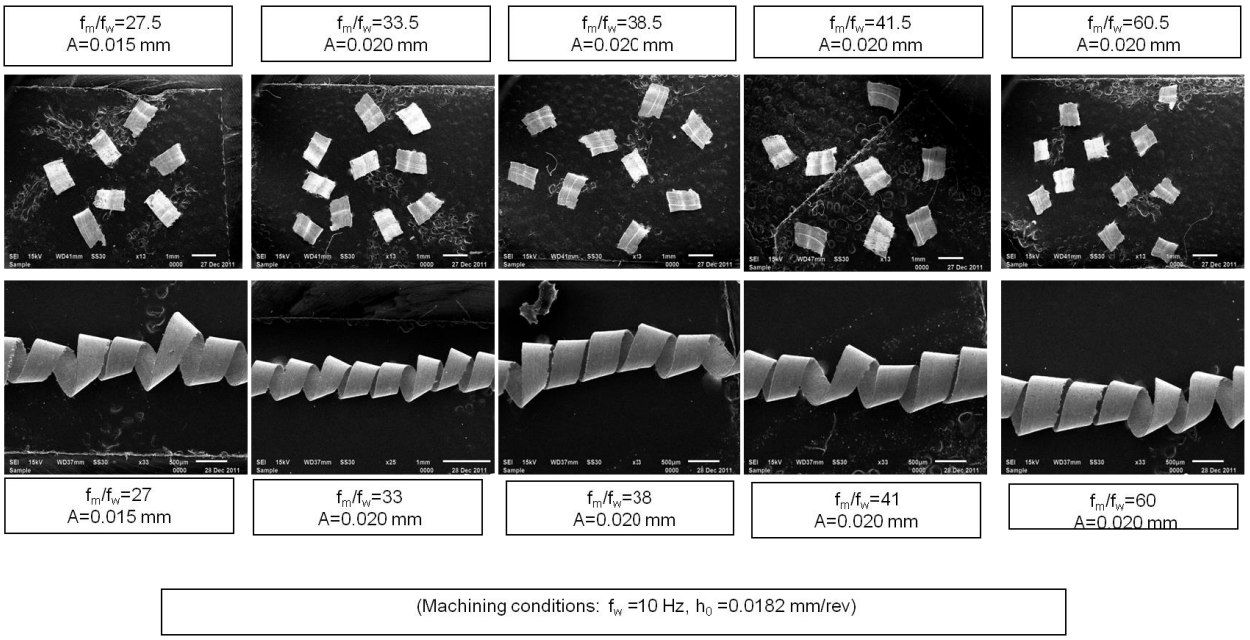


Figure 4: SEM morphology of chips generated at increasing values of f_m/f_w ratio during modulation assisted machining (MAM) of brass (f_m refers to frequency of modulation, f_w frequency of wokpiece rotation and A amplitude of modulation)

Table II shows the full width at half-maximum (FWHM) value of the peaks at specific 2 theta angle for the particulates produced at different f_m/f_w ratios. For simplicity, the particulates produced at f_m/f_w = 27.5, 33.5, 38.5, 41.5 and 60.5 are designated as A, B, C, D and E respectively. The XRD profiles of chip particulates A, B, C, D and E are shown in Fig. 5. The results show that the change in f_m/f_w has a very little effect on the internal strain in the particulates produced at different f_m/f_w ratios. For A and B types of chip particulates, the

https://doi.org/10.1017/S088571561300095X Published online by Cambridge University Press

crystallite size was calculated as 11.5 nm, whereas for C-E types of particulates, the crystallite size was 12 nm. On the other hand, a crystallite size of 25 nm was found for the bulk brass. A maximum microstrain of 0.037 was found for the type D particulates, whereas a minimum value of 0.0316 was observed for type- C chips. It can be concluded from the analysis that the chips of types A-E have smaller crystallite size and higher microstrain as compared to bulk brass. It is pertinent to mention that there is no noticeable difference in microstrain and crystallite size of A-E type particulates produced at different f_m/f_w ratios.

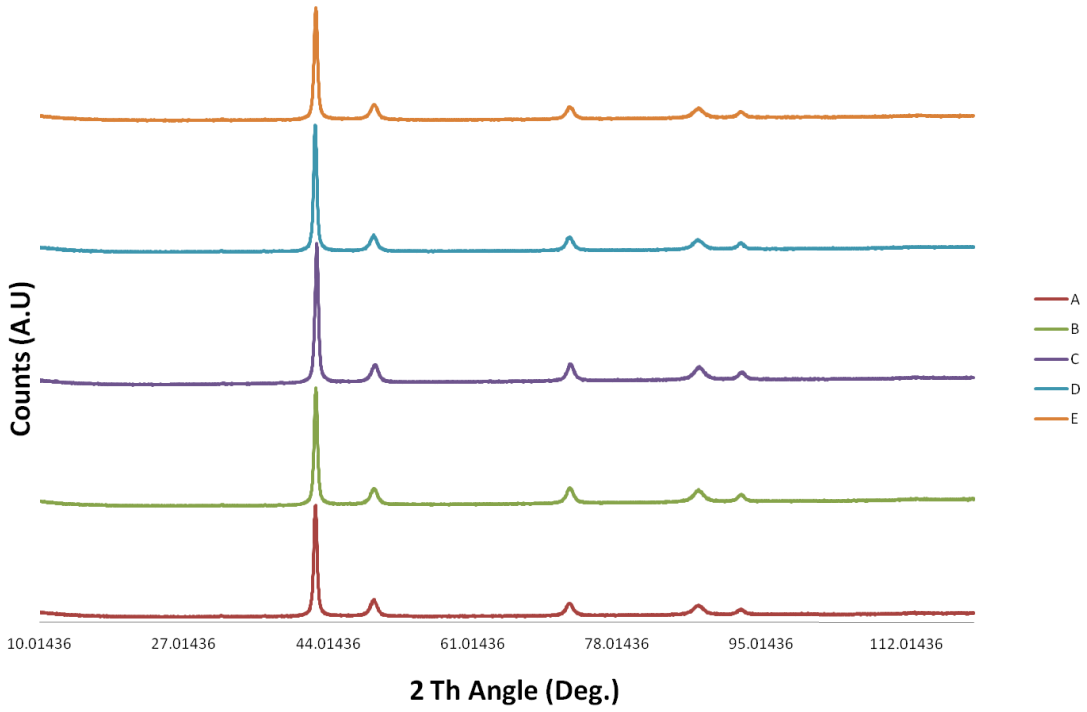


Figure 5: Peak profile of different chip particulates produced at different f_m/f_w during modulation assisted machining of brass

https://doi.org/10.1017/S088571561300095X Published online by Cambridge University Press

Table II: Strain-size data investigated of chip particulates produced at different f_m/f_w ratio obtained from X-ray diffraction						
	Pos. 2 Th (Deg)	Height [cts]	FWHM 2Th (deg)	Area [cts*°2Th.]	Microstrain	Crystallite size (nm)
A						
1	42.4769	7813	0.443	5014.74	0.0346	11.5
2	49.319	1040	0.964	1575.11		
3	72.374	811	1	1107.15		
4	87.478	653	1.41	1444.18		
B						
1	42.4143	8830	0.413	5307.73	0.0347	11.5
2	49.264	1032	0.97	1550.49		
3	72.331	907	0.95	1228.78		
4	87.443	648	1.42	1403.75		
C						
1	42.4788	8154	0.429	5023.49	0.0316	12
2	49.313	1098	0.95	1646.94		
3	72.375	1041	0.937	1398.88		
4	87.48	793	1.35	1656.76		
D						
1	42.4335	7730	0.427	4742.48	0.037	12
2	49.278	1075	0.951	1544.62		
3	72.33	839	0.95	1153.61		
4	87.437	631	1.43	1385.07		
E						
1	42.5811	9598	0.429	5959.17	0.032	12
2	49.409	1179	0.95	1746.72		
3	72.451	1133	0.9	1481.85		
4	87.563	863	1.36	1820.73		

https://doi.org/10.1017/S088571561300095X Published online by Cambridge University Press

IV. CONCLUSION

MAM is a promising technique for the fabrication of brass powder particles of uniform sizes and shapes. In the current work, the particulates in the size range of 5 mm - 100 µm were produced by this process. Variation in size of particles was around 5%. It is concluded that with a decrease in chip particulate size, the crystallite size also decreases, while the internal strain increases. With an increase in value of f_m/f_w ratio, the chip lengths become increasingly smaller; however, there is no noticeable difference in microstrain and crystallite size of these chips. In comparison to the bulk brass, the chips produced at different f_m/f_w ratios were found to have smaller crystallite size, however with increased microstrain. This change in crystallite size and microstrain may be attributed to the severe plastic deformation taking place during MAM. This SPD increases the defects in chip particulates, thereby changing the microstrain and the crystallite size of the particulates.

Biju, V., Sugathan, N., Vrinda, V. and Salini, S. (**2008**). "Estimation of lattice strain in nanocrystalline silver from X-ray diffraction line broadening," J.Mater. Sci. **43**(4): 1175-1179.

Joshi, R. S. and Singh, H. (**2011**). "Piezoelectric transducer based devices for development of a sustainable machining system - A review," Applications of Ferroelectrics. International Symposium 2011 (ISAF/PFM) (and 2011 International Symposium on Piezoresponse Force Microscopy and Nanoscale Phenomena in Polar Materials).

Lemine, O. M. (**2009**). "Microstructural characterisation of nanoparticles using, XRD line profiles analysis, FE-SEM and FT-IR," Superlattices Microstruct. **45**(6), 576-582.

Lenel, F. V. (**1980**). *Powder Metallurgy: Principles and Applications*, (Metal Powder Industries Federation, Princeton, NJ).

Lonardelli, I., Almer, J., Ischia, G., Menapace and C. Molinari, A. (**2009**). "Deformation behavior in bulk nanocrystalline-ultrafine aluminum: in situ evidence of plastic strain recovery," Scr. Mater. **60**(7), 520-523.

Mann, J. B., Chandrasekar, S. and Compton, W. D. (**2009**). *Tool Holder Assembly and Method for Modulation-Assisted Machining*. US Patent no 7,587, 965 B2.

Mann, J. B., Saldana, C., Chandrasekar, S., Compton, W. D. and Trumble, K. P. **(2007)**. "Metal particulate production by modulation-assisted machining." Scr. Mater. **57**(10): 909-912.

https://doi.org/10.1017/S088571561300095X Published online by Cambridge University Press

Pourghahramani, P., Altin, E., Mallembakam, M. R., Peukert, W. and Forssberg, E. (**2008**). "Microstructural characterization of hematite during wet and dry millings using Rietveld and XRD line profile analyses," Powder Technol. **186**(1), 9-21.

Sánchez, L. C., Arboleda, J. D., Saragovi, C., Zysler, R. D. and Barrero, C. A. (**2007**). "Magnetic and structural properties of pure hematite submitted to mechanical milling in air and ethanol," Phys. B (Amsterdam, Neth.) **389**(1), 145-149.

Ungar, T., J., Gubicza, J., Ribarik, G. and Borbely, A. (**2001**). "Crystallite size distribution and dislocation structure determined by diffraction profile analysis: principles and practical application to cubic and hexagonal crystals," Journal Appl. Crystallogr. **34**(3), 298-310.

Williamson, G. K. and Hall, W. H. (**1953**). "X-Ray Line Broadening from Filed Aluminium and Wolfram, " Acta Metall. **1**, 22-31.

https://doi.org/10.1017/S088571561300095X Published online by Cambridge University Press